

# Overabundance of s-process elements in the atmosphere of the active red giant PZ Mon<sup>\*</sup>

Yu. V. Pakhomov,<sup>1</sup>

<sup>1</sup>*Institute of Astronomy, Russian Academy of Sciences, Pyatnitskaya 48, 119017, Moscow, Russia*

26 September 2018

## ABSTRACT

Based on high-resolution ( $R=60\,000$ ) spectra taken with the NES spectrograph (the 6-m BTA telescope, the Special Astrophysical Observatory of the Russian Academy of Science), we have determined the abundances of 26 elements, from lithium to europium, in the atmosphere of the active red giant PZ Mon which belongs to the class of RS CVn variable stars, by the method of model stellar atmospheres. We have taken into account the hyperfine splitting, the isotopic shift, and the departure from local thermodynamic equilibrium. Analysis of our data has revealed an overabundance of lithium and neutron-capture elements compared to normal red giants. For lithium, this is explained by the activity of the star, while the overabundance of s-elements is presumably similar in nature to that in moderate barium stars.

**Key words:** stars: individual: PZ Mon – (stars:) binaries: spectroscopic – (stars:) starspots – stars: variables: general

## 1 INTRODUCTION

PZ Mon (HD 289114) is an RS CVn variable binary star whose components are represented by a red giant of spectral type K2III (Pakhomov et al. 2015) and a red dwarf of spectral type M7V (Pakhomov & Gorynya 2015). Previously (Pakhomov et al. 2015), we determined the parameters of the stellar atmosphere for the primary component of PZ Mon by various independent methods, its effective temperature  $T_{eff}=4700\pm 100$  K and surface gravity  $\log g=2.8\pm 0.2$ , and revealed the signatures of chromospheric activity based on optical and ultraviolet observations and a corona based on X-ray observations. The optical variability ( $\Delta m \approx 0.03^m$ ) of the star is caused by a nonuniform distribution of temperature spots on its surface: a large fraction of them is concentrated on the side facing the secondary component, about 24% of the surface is covered with spots, while their fraction on the opposite side is about 20% (Aleksiev & Bondar' 2006).

The binary system PZ Mon is interesting in many aspects. The rotation velocity of the primary component,  $v_{rad}=10.5$  km s<sup>-1</sup>, exceeds the typical rotation velocities of red giants, 3–5 km s<sup>-1</sup>. The component mass ratio,  $M_2/M_1 = 0.14M_{\odot}:1.5M_{\odot} = 0.09$ , is minimal among the known RS CVn giants. At the same time, the binary system rotates synchronously with a period of 34.13 days, while all

such binary systems similar in parameters are asynchronous (Pakhomov & Gorynya 2015), which raises the question about the synchronization mechanism of PZ Mon. Thus, a comprehensive study of the star PZ Mon is topical, including a comparative analysis of the chemical composition that can set PZ Mon apart from the normal red giants and active RS CVn giants.

In this paper, we have determined the abundances of 26 elements in the atmosphere of PZ Mon for the first time to perform a comparative analysis of this active giant with other RS CVn giants and normal red giants of the Galactic thin disk. These data will subsequently be used to calculate the distribution of temperature spots on the surface of the star being investigated by the method of Doppler tomography and to study the influence of the secondary component on the activity of the primary one.

## 2 OBSERVATIONS

The spectroscopic observations of PZ Mon were performed on February 10, 2015, with the NES spectrograph mounted at the Nasmyth focus of the 6-m BTA telescope at the Special Astrophysical Observatory of the Russian Academy of Sciences. The regime of observations with an image slicer was used; the spectral resolution was  $R=60\,000$ . Three consecutive half-hour exposures were taken on an e2v CCD42-90 (4632×2068 pix). We applied the MIDAS software package to process the spectra. We extracted 54 echelle orders in the

<sup>\*</sup> Based on observations collected at the BTA telescope (Special Astrophysical Observatory, Russia)

**Table 1.** Abundances of chemical elements in the atmosphere of PZ Mon:  $N$  is the number of lines used,  $[E/H]$  and  $\sigma[E/H]$  are the relative abundance and its error, hfs stands for hyperfine splitting, iso stands for isotopic shift, nLTE means that LTE is abandoned.

Element	$N$	$[E/H]$	$\sigma[E/H]$	Remark
Li1	1	0.46	0.07	hfs, iso, nLTE
C1	3	-0.26	0.07	
N1	1	0.25	0.15	
O1	1	0.14	0.08	
Na1	2	0.19	0.02	hfs, nLTE
Mg1	2	0.04	0.10	nLTE
Al1	1	0.00	0.03	hfs, nLTE
Si1	9	0.04	0.09	
Ca1	6	0.05	0.08	
Sc1	4	0.07	0.05	hfs
Sc2	4	0.19	0.10	hfs
Ti1	26	0.07	0.08	
Ti2	3	0.07	0.03	
V1	23	0.09	0.07	hfs
Cr1	11	0.11	0.08	
Mn1	5	0.13	0.11	hfs
Fe1	90	0.08	0.09	
Fe2	4	0.17	0.10	
Co1	11	0.06	0.11	hfs
Ni1	14	0.04	0.08	
Sr1	1	0.15	0.11	
Y1	1	0.09	0.03	hfs
Y2	2	0.18	0.06	hfs
Zr1	4	-0.02	0.09	
Mo1	1	0.18	0.10	
Ba2	3	0.58	0.10	hfs, iso, nLTE
La2	1	0.39	0.04	hfs
Ce2	2	0.37	0.03	
Nd2	4	0.57	0.08	
Eu2	1	0.22	0.08	hfs, iso

spectral range from 3890 to 6980 Å. The wavelength calibration was based on the spectrum of a thorium-argon lamp. The preprocessing of the spectra also included the removal of cosmic-ray particle hits and allowance for the scattered light. An arbitrary echelle order consists of three separate spectra: the main spectrum and two spectra from the image slicer, which were processed separately. At the end of the processing procedure, the signal from the slicer was added to the main spectrum. Each of the three exposures of the spectrum for PZ Mon was also processed separately, and all spectra were then added with allowance made for the difference in the Earth’s projected rotation velocity. The mean signal-to-noise ratio in the resulting spectrum was about of 120. The spectrum was normalized to the continuum level using the blaze function obtained from the flat field spectrum and using the synthetic spectrum of a star with model parameters similar to those of PZ Mon. Our primary analysis of the spectrum allowed us to determine the radial velocity  $v_{\text{rad}}=23.91\pm 0.16 \text{ km s}^{-1}$ .

**Table 2.** The errors in the elemental abundances determined by changing the effective temperature (+100 K), surface gravity (+0.2), and microturbulent velocity (+0.15  $\text{km s}^{-1}$ ) and the total root-mean-square error

Ion	$\Delta E/H$			total
	$\Delta T_{eff}(+100 \text{ K})$	$\Delta \log g(+0.2)$	$\Delta v_{mic}(+0.15 \text{ km s}^{-1})$	
Li1	0.15	0.00	-0.02	0.15
C1	-0.02	0.04	-0.01	0.05
N1	0.12	0.06	0.00	0.13
O1	0.01	0.08	0.00	0.08
Na1	0.08	-0.02	-0.05	0.10
Mg1	0.03	-0.01	-0.03	0.04
Al1	0.07	0.00	-0.01	0.07
Si1	-0.05	0.04	-0.02	0.07
Ca1	0.10	-0.03	-0.07	0.13
Sc1	0.15	0.01	-0.03	0.15
Sc2	-0.01	0.08	-0.05	0.09
Ti1	0.14	0.00	-0.05	0.15
Ti2	-0.02	0.08	-0.07	0.11
V1	0.17	0.01	-0.07	0.18
Cr1	0.11	0.00	-0.04	0.12
Mn1	0.10	-0.00	-0.09	0.13
Fe1	0.04	0.02	-0.06	0.07
Fe2	-0.11	0.12	-0.04	0.17
Co1	0.04	0.04	-0.07	0.09
Ni1	0.03	0.03	-0.08	0.09
Sr1	0.19	0.00	-0.13	0.23
Y1	0.18	0.00	-0.04	0.18
Y2	-0.01	0.09	-0.01	0.09
Zr1	0.18	0.01	-0.04	0.18
Mo1	0.14	0.00	-0.02	0.14
Ba2	0.03	0.02	-0.06	0.07
La2	0.02	0.09	-0.02	0.09
Ce2	0.00	0.08	-0.01	0.08
Nd2	0.01	0.08	-0.03	0.09
Eu2	0.00	0.09	-0.01	0.09

### 3 DETERMINING THE ABUNDANCES OF CHEMICAL ELEMENTS

We analyzed the spectrum by the synthetic spectrum method in the Binmag3 code (written by O. Kochukhov<sup>1</sup>). For our calculations of the theoretical spectra, we used the Synth3 and the model stellar atmosphere with parameters  $T_{eff}=4700\pm 100 \text{ K}$ ,  $\log g=2.8\pm 0.2$ , and  $v_{mic}=1.3 \text{ km s}^{-1}$  computed with the ATLAS9 code (Kurucz 1993). The list of atomic and molecular spectral lines for the Synth3 code was retrieved from the VALD3 database (Ryabchikova et al. 2015) using the “select stellar” function, which allows one to select only those lines in a given wavelength range whose intensity exceeds a given threshold value and will be sufficient for them to be visible in the spectrum. The synthetic spectrum includes 25 123 lines in the range from 4000 to 7000 Å with an intensity differing from the continuum intensity by more than 0.01. From this list we selected the lines with a minimal degree of blending with neighboring lines to determine the abundances of chemical elements from the condition:

$$F^{cen} < 0.05 F^{blend}$$

<sup>1</sup> <http://www.astro.uu.se/~oleg/binmag.html>

where

$$F^{blend} = \sum_{i=1}^N F_i^{cen} e^{-\frac{(\lambda-\lambda_i)^2}{\Delta\lambda^2}}$$

$$\Delta\lambda = \sqrt{(\lambda v_{rot} \sin i/c)^2 + (\lambda/R)^2}$$

where  $F^{cen}$  is the central depth of the spectral line,  $F^{blend}$  is the estimated depth of the spectrum at the center of the line being investigated with wavelength  $\lambda$  formed by  $N$  neighboring lines with wavelengths  $\lambda_i$ ,  $\Delta\lambda$  is the characteristic width of the spectral line,  $v_{rad}=10.5 \text{ km s}^{-1}$  is the rotation velocity of PZ Mon  $\sin i=0.92$  is the inclination of the rotation axis of PZ Mon,  $c$  is the speed of light, and  $R=60\,000$  is the spectral resolution. The blending was taken into account around each line at a distance of  $5\Delta\lambda$ . From the produced list of lines we then selected only those that could be measured with a high quality in the observed spectrum of the star being investigated. The final list includes 294 spectral lines.

To determine the abundances of chemical elements, we applied the Levenberg–Marquardt method of fitting the theoretical spectrum to the observed one. The variation parameters were the elemental abundance  $\log(\text{El}/\text{H})$ , the radial velocity  $v_{rad}$ , and the macroturbulent velocity  $v_{mac}$ . The quality of the fit was controlled by the condition under which the difference of the theoretical and observed spectra was below the noise level. We separately calculated the profile of a specific spectral line to analyze the degree of influence of the neighboring lines. All of the measured lines in the spectrum of PZ Mon were also measured in the NAO solar spectrum (Kurucz et al. 1984) for the subsequent calculation of differential abundances to reduce the systematic errors in atomic parameters.

The hyperfine splitting (HFS) effect was taken into account using the hyperfine structure constants  $A$  and  $B$  for the atomic levels of odd isotopes of sodium, aluminum, scandium, vanadium, manganese, cobalt, yttrium, barium, lanthanum, and europium<sup>2</sup>. For this purpose, we wrote a code that analyzed the input list of spectral lines to calculate the synthetic spectrum, checked the availability of the necessary data (identified the lower and upper transition levels, sought for the coefficients  $A$  and  $B$ ), and launched the calculation of the wavelengths and intensities of the HFS components. As a result, each unsplit line from the input list having data on its splitting was replaced by a set of lines according to the number of components with the logarithms of their oscillator strengths  $\log gf_0 + \log(I_i) - \log(\sum I_i)$ , where  $\log gf_0$  is the oscillator strength of the unsplit line,  $I_i$  is the relative intensity of the  $i$ -th component, and  $\sum I_i$  is the sum of the intensities of all splitting components.

For lithium, we used the available data on the HFS and isotopic shift by Smith et al. (1998). For barium, we performed our calculations separately for each isotope and then added the values corresponding to the logarithm of the relative isotope abundance (Rosman & Taylor 1998) to the oscillator strengths. We took into account the departure from local thermodynamic equilibrium (LTE) using non-LTE corrections: from Lind et al. (2009) for lithium,

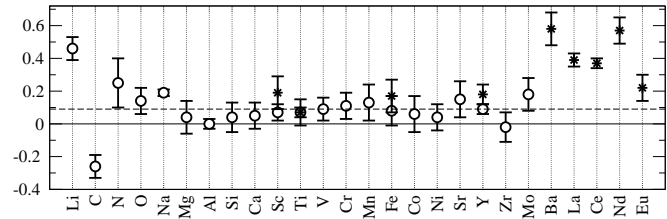


**Figure 1.** Abundances of chemical elements in the atmosphere of PZ Mon. The circles and asterisks denote the elements whose abundances were determined from the spectral lines of neutral atoms and ions, respectively. The dashed line marks the metallicity level determined from iron-peak elements.

from Alexeeva et al. (2014) and Liu et al. (2007) for sodium, magnesium, and aluminum, and from Mashonkina & Zācs (1996) for barium.

The results are presented in Table 1: the first column gives the element and its ionization stage from  $N$  lines (the second column) of which the relative abundance  $[\text{El}/\text{H}]$  (the third column) and its error  $\sigma[\text{El}/\text{H}]$  (the fourth column), which also takes into account the accuracy of fitting the line profiles, were determined; the last column gives the effects that were taken into account for the lines of the specified element. In the case of nitrogen, the error in the abundance being determined allows for the error in the carbon abundance, because nitrogen bonds with carbon into CN molecular lines. These data are also shown in Fig. 1, where the circles and asterisks denote the elements whose abundances were determined from the lines of neutral atoms and ions, respectively.

To illustrate the reliability of the measurement results, Fig. 2 compares the observed and synthetic profiles for some spectral lines that are difficult to measure and the profiles when changing the elemental abundance by  $\pm 0.10$ . The lithium abundance was derived from one 6707 Å line at a distance of 4 Å from the edge of the echelle order. The line in the spectrum from Pakhomov et al. (2015) was located slightly farther, but the signal-to-noise ratio was smaller. Therefore, in this paper, we averaged the abundances derived by analyzing the previous (-10.31) and present (-10.46) spectra. When describing the lithium lines, we took into account the cyanogen molecular lines. We estimated the carbon and nitrogen abundances by CH (4835 Å), C<sub>2</sub> (5086 Å 5135 Å), and CN (6250–6251 Å) molecular lines. The first line is located in the region of the spectrum where the continuum is difficult to draw and gives a low abundance, C/H=3.80. The C<sub>2</sub> lines are very sensitive to the carbon abundance and give similar results, C/H=-3.70 and -3.64, respectively. The 6300 Å line was the only possible one for determining the oxygen abundance. This line is blended with two lines of nickel isotopes ( $\lambda_1=6300.335 \text{ Å}$ ,  $\log gf_1 = -2.25$  and  $\lambda_2=6300.355 \text{ Å}$ ,  $\log gf_2 = -2.67$ ), a weak iron line, and the scandium line with HFS affects the line wings. The strontium and molybdenum abundances were measured from the 4607.33 and 5506.45 Å by taking into account the possible blends.

Table 2 presents the results of our analysis of the errors in the abundances of chemical elements. The first column gives the ion name, the next three columns give the changes in elemental abundance when changing the effective temper-

<sup>2</sup> <http://kurucz.harvard.edu/atoms.html>

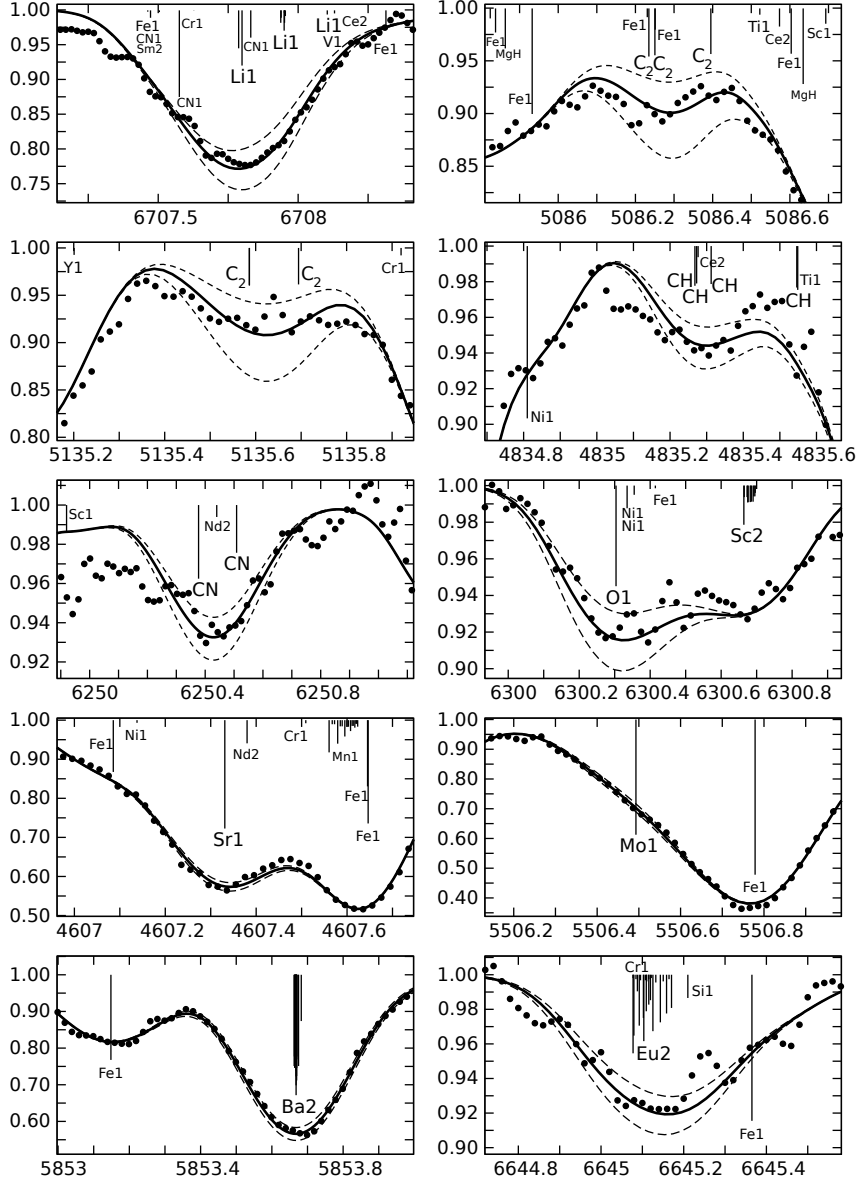


**Figure 2.** Li1, C<sub>2</sub>, CH, CN, O1, Sr1, Mo1, Ba2, and Eu2 line profiles. The dots indicate the observed spectrum, the thick line indicates the best fit synthetic spectrum, the dotted line indicates the profile when changing the abundance of a given element by  $\pm 0.10$ , and the vertical lines indicate the relative contribution to the synthetic spectrum from various lines.

ature by 100 K, the surface gravity by 0.2 dex, and the microturbulent velocity by  $0.15 \text{ km s}^{-1}$ , the last column gives the total error calculated as the root-mean-square error.

#### 4 DISCUSSION

Since RS CVn stars have temperature spots on the surface, we estimated their influence on the observed spectrum of PZ Mon. Our calculations of the theoretical fluxes (the Synth3 code) show that the stellar continuum intensity in the range 5000–6000 Å for an effective temperature of 4700 K is a factor of 5–6 higher than that for a spot temperature of 3500 K (we took the minimum temperature of the ATLAS9 models). At the star’s filling factor of 0.25 (the ratio of the spot area to the entire visible disk area), the dif-

ference between the intensities of the surface of a star with and without spots will reach a factor of 15–18. The presence of such a small number of spots will manifest itself as a reduction in the continuum level, forming a pseudo-continuum relative to which the line intensities barely change: the calculated differences are smaller than the noise of the observed spectrum. If the spot temperature is even lower, as was pointed out by Alekseev & Bondar’ (2006), then the influence of spots on the observed spectrum will be even smaller. The degree of influence of spots can also be estimated from the presence or absence of strong TiO molecular bands typical for a stellar atmosphere with a temperature below 4000 K. There are no TiO molecular lines, including those in the strong 6158 Å band, in the spectrum of PZ Mon. Therefore, we analyzed the abundances of chemical elements without allowance for the spottedness. We also analyzed the

widths of spectral lines depending on their Lande factors. However, no such dependence was found; therefore, we disregarded the magnetic field in our calculations.

Because of the cool atmosphere and the fairly high rotation velocity ( $10.5 \text{ km s}^{-1}$ ), there are few unblended lines in the spectrum of PZ Mon. For most rare-earth elements, we still had to use the line profile measurements by taking into account the blends (Fig. 2). It can be seen from Fig. 1 and Table 1 that the metallicity determined from iron-peak elements is  $0.09 \pm 0.09$ , and most elements have a relative abundance close to this value.

Lithium ( $\text{Li}/\text{H} = -10.38$ ,  $A(\text{Li}) = 1.62$ ) shows a considerable overabundance both relative to the solar value ( $\text{Li}/\text{H} = -10.84$ ,  $A(\text{Li}) = 1.16$ ) and relative to the normal red giants in the spectra of which lithium is represented by a weak line or is not observed at all (Liu et al. 2014). The absence of lithium is explained by its depletion in the shell into which it is transferred by the red giant's extensive convective envelope. The presence of lithium in the atmospheres of some giants is associated with their activity (Fekel & Balachandran 1994), a high rotation velocity (Fekel & Balachandran 1993; Carlberg et al. 2013), and even the presence of planets (Liu et al. 2014). Active RS CVn stars, to which the star PZ Mon being investigated belongs, generally exhibit a lithium overabundance (Liu et al. 1993; Morel et al. 2003). The derived carbon (underabundance), nitrogen (overabundance), and oxygen (normal) abundances are typical for normal red giants and reflect the result of the first dredge-up (Lambert & Ries 1981). For the same reason, sodium also has a slight overabundance, which is observed in red giants of various groups (Antipova et al. 2005; Alexeeva et al. 2014).

Figure 1 shows an overabundance of slow-neutron capture elements, with the mean abundance of light *s*-elements (ls: Sr, Zr, Y, Mo) relative to iron  $[\text{ls}/\text{Fe}] = 0.04 \pm 0.12$  being appreciably smaller than the mean relative abundance of heavy *s*-elements (hs: Ba, La, Ce, Nd)  $[\text{hs}/\text{Fe}] = 0.40 \pm 0.14$ . The fact that the abundances of light *s*-elements were determined from the lines of neutral atoms, for which the effect of departure from LTE reducing the line intensity is significant, while those of heavy ones were determined from ions in the first dominant ionization stage, for which the effect of departure from LTE may be neglected, can be responsible for such a difference. The spectral lines of light *s*-elements in the second ionization stage are mostly in the blue part of the spectrum, where the spectrum of PZ Mon exhibits a strong blending due to the influence of molecular lines and a high rotation velocity; therefore, we did not use them. The effect of departure from LTE on the abundance being determined can be significant. For example, it is  $\sim 0.3$  dex for zirconium (Velichko et al. 2010). However, for the zirconium, strontium, and molybdenum lines being used, the non-LTE corrections are difficult to estimate due to the absence of such data. Thus, the observed difference in the abundances of heavy and light *s*-elements  $[\text{hs}/\text{ls}] = 0.36$  can be explained by the effect of departure from LTE, while the overabundance of  $[\text{s}/\text{Fe}]$  itself can be, on average, 0.3–0.4 dex. An overabundance of *s*-elements was detected in the atmospheres of classical barium and CH stars. However, they also exhibit a carbon overabundance, in contrast to PZ Mon. Moderate barium stars have a slight overabundance of  $[\text{s}/\text{Fe}]$  at normal relative abundances of other elements (Pilachowski 1977; Boyarchuk et al. 2002; Smiljanic et al. 2007). An over-

abundance of *s*-elements is not typical for RS CVn stars. Morel et al. (2003) investigated the chemical composition of six active RS CVn giants, and only one of them has the abundance  $[\text{Ba}/\text{Fe}] = 0.34$ . Basak et al. (2010) found no differences in the abundances of neutron-capture elements in the atmospheres of more than 30 active (RS CVn and BY Dra) and nonactive stars. Consequently, the moderate overabundance of *s*-elements in the atmosphere of PZ Mon is a characteristic of this star itself.

The nature of moderate barium stars is not completely clear. These can be red giants at a later evolutionary stage (Boyarchuk et al. 2002) and binary stars with a relatively large separation of the components (Bohm-Vitense et al. 1984). The binarity of some moderate barium stars was discovered by the radial velocities (Udry et al. 1998, Udry et al. 1998); their periods ( $P$ ) are thousands of days, while the masses of the secondary components are close to the solar mass, which is much larger than that for PZ Mon but the ratios  $M_2/\sqrt{P}$  are very close. In addition, X-ray sources are encountered among the moderate barium stars (Jorissen et al. 1996), which may be indicative of their activity. Thus, the nature of the overabundances of *s*-elements in the atmosphere of PZ Mon may be similar to the nature of those in moderate barium stars, but it is not typical for all RS CVn stars and requires a more detailed study.

## 5 CONCLUSIONS

We determined the abundances of 26 chemical elements in the atmosphere of the active red giant PZ Mon by the method of model stellar atmosphere by taking into account the hyperfine splitting, the isotopic shift, and (for some elements) the departure from LTE through non-LTE corrections. Analysis of our data showed that the abundances of most elements are typical for normal red giants, except for lithium whose overabundance is characteristic for rapidly rotating and active RS CVn stars and the neutron-capture elements whose overabundance may be the same in nature as that in the atmospheres of moderate barium stars.

## ACKNOWLEDGMENTS

This work was supported in part by the Russian Foundation for Basic Research (project no. 15-02-06046) and the Program of the Presidium of the Russian Academy of Sciences “Nonstationary Phenomena in the Universe”.

## REFERENCES

- Alekseev I., Bondar' N., 2006, *Astronomical and Astrophysical Transactions*, 25, 247
- Alexeeva S. A., Pakhomov Y. V., Mashonkina L. I., 2014, *Astronomy Letters*, 40, 406
- Antipova L. I., Boyarchuk A. A., Pakhomov Y. V., Yushkin M. V., 2005, *Astronomy Reports*, 49, 535
- Basak N. Y., Mishenina T. V., Soubiran C., Kovtyukh V. V., Belik S. I., 2010, *Odessa Astronomical Publications*, 23, 17

- Bohm-Vitense E., Nemeč J., Proffitt C., 1984, *ApJ*, 278, 726
- Boyarchuk A. A., Pakhomov Y. V., Antipova L. I., Boyarchuk M. E., 2002, *Astronomy Reports*, 46, 819
- Carlberg J. K., Cunha K., Smith V. V., Majewski S. R., 2013, *Astronomische Nachrichten*, 334, 120
- Fekel F. C., Balachandran S., 1993, *ApJ*, 403, 708
- Fekel F. C., Balachandran S., 1994, in Caillault J.-P., ed., *Cool Stars, Stellar Systems, and the Sun Vol. 64 of Astronomical Society of the Pacific Conference Series, Lithium in Chromospherically Active Giants*. p. 279
- Jorissen A., Schmitt J. H. M. M., Carquillat J. M., Ginestet N., Bickert K. F., 1996, *A&A*, 306, 467
- Kurucz R., 1993, *ATLAS9 Stellar Atmosphere Programs and 2 km/s grid*. Kurucz CD-ROM No. 13. Cambridge, Mass.: Smithsonian Astrophysical Observatory, 1993., 13
- Kurucz R. L., Furenlid I., Brault J., Testerman L., 1984, *Solar flux atlas from 296 to 1300 nm*
- Lambert D. L., Ries L. M., 1981, *ApJ*, 248, 228
- Lind K., Asplund M., Barklem P. S., 2009, *A&A*, 503, 541
- Liu X.-f., Zhao G., Tan H.-s., Lu F.-j., 1993, *Chinese Astron. Astrophys.*, 17, 51
- Liu Y. J., Tan K. F., Wang L., Zhao G., Sato B., Takeda Y., Li H. N., 2014, *ApJ*, 785, 94
- Liu Y. J., Zhao G., Shi J. R., Pietrzyński G., Gieren W., 2007, *MNRAS*, 382, 553
- Mashonkina L. I., Začs L., 1996, *Ap&SS*, 236, 185
- Morel T., Micela G., Favata F., Katz D., Pillitteri I., 2003, *A&A*, 412, 495
- Pakhomov Y. V., Chugai N. N., Bondar' N. I., Gorynya N. A., Semenko E. A., 2015, *MNRAS*, 446, 56
- Pakhomov Y. V., Gorynya N. A., 2015, *Astronomy Letters*, 41, 677
- Pilachowski C. A., 1977, *A&A*, 54, 465
- Rosman K. J. R., Taylor P. D. P., 1998, *Journal of Physical and Chemical Reference Data*, 27, 1275
- Ryabchikova T., Piskunov N., Kurucz R. L., Stempels H. S., Heiter U., Pakhomov Y., Barklem P., 2015, *Phys. Scr*, 90, 4005
- Smiljanic R., Porto de Mello G. F., da Silva L., 2007, *A&A*, 468, 679
- Smith V. V., Lambert D. L., Nissen P. E., 1998, *ApJ*, 506, 405
- Udry S., Jorissen A., Mayor M., Van Eck S., 1998, *A&AS*, 131, 25
- Udry S., Mayor M., Van Eck S., Jorissen A., Prevot L., Grenier S., Lindgren H., 1998, *A&AS*, 131, 43
- Velichko A. B., Mashonkina L. I., Nilsson H., 2010, *Astronomy Letters*, 36, 664